J|A|C|S
ARTICLES
Published on Web 04/28/2007

Crucial Role of Anions on the Deprotonation of the Cationic Dihydrogen Complex *trans*-[FeH(η^2-H_2)(dppe)$_2$]$^+$

Manuel G. Basallote,*[,†] Maria Besora,[‡] C. Esther Castillo,[†] María J. Fernández-Trujillo,[†] Agustí Lledós,*[,‡] Feliu Maseras,[‡,§] and M. Angeles Máñez[†]

Contribution from the Departament de Química, Edifici Cn, Universitat Autònoma de Barcelona, 08193 Bellaterra, Barcelona, Catalonia, Spain, Institut Català d'Investigacions Químiques, ICIQ, Avenida Països Catalans 16, 43007 Tarragona, Catalonia, Spain, and Departamento de Ciencia de los Materiales e Ingeniería Metalúrgica y Química Inorgánica, Facultad de Ciencias, Universidad de Cádiz, Apartado 40, Puerto Real, 11510 Cádiz, Spain

Received February 9, 2007; E-mail: manuel.basallote@uca.es; agusti@klingon.uab.es

Abstract: The kinetics of reaction of the dihydrogen complex *trans*-[FeH(η^2-H_2)(dppe)$_2$]$^+$ with an excess of NEt_3 to form *cis*-[FeH_2(dppe)$_2$] shows a first-order dependence with respect to both the metal complex and the base. The corresponding second-order rate constant only shows minor changes when the solvent is changed from THF to acetone. However, the presence of salts containing the BF_4^-, PF_6^-, and BPh_4^- anions causes larger kinetic changes, the reaction being accelerated by BF_4^- and PF_6^- and decelerated in the presence of BPh_4^-. These results can be interpreted considering that the ion pairs formed by the complex and the anion provide a reaction pathway more efficient than that going through the unpaired metal complex. From the kinetic results in acetone solution, the stability of the ion pairs and the rate constant for their conversion to the reaction products have been derived. Theoretical calculations provide additional information about the reaction mechanism both in the absence and in the presence of anions. In all cases, the reaction occurs with proton transfer from the *trans*-dihydride to the base through intermediate structures showing Fe—H_2···N and Fe—H···H···N dihydrogen bonds, isomerization to the cis product occurring once the proton transfer step has been completed. Optimized geometries for the ion pairs show that the anions are placed close to the H_2 ligand. In the case of BPh_4^-, the bulky phenyls hinder the approach of the base and make the ion pairs unproductive for proton transfer. However, ion pairs with BF_4^- and PF_6^- can interact with the base and evolve to the final products, the anion accompanying the proton through the whole proton transfer process, which occurs with an activation barrier lower than for the unpaired metal complex.

Introduction

Counteranions accompanying cationic metal complexes in their salts are usually selected to behave as inert species in reaction media. To safely assume that they do not participate in chemical reactions, anions of low coordinating power are preferentially used. The same reasoning is also used when selecting the salts added as supporting electrolytes in quantitative equilibrium and kinetic solution studies. Nevertheless, some striking effects of anions on the solution reactivity of metal complexes have been reported in several recent investigations.[1−5] In most cases, the active role of the anions has its origin in the formation of ion pairs with the reactants and/or the products. Macchioni has recently published a thorough review on the ion pairing effects in transition metal organometallic chemistry.[6]

We have previously studied the role of ion pairs in the reactions of proton transfer to hydride transition metal complexes ([M]—H) from proton donors of moderate acidity.[7−9] Protonation of [M]—H to form dihydrogen complexes has been the subject of intensive work,[10−14] and the mechanism nowadays accepted

† Universidad de Cádiz.
‡ Universitat Autònoma de Barcelona.
§ Institut Català d'Investigacions Químiques.

(1) Appelhans, L. N.; Zuccaccia, D.; Kovacevic, A.; Chianese, A. R.; Miecznikowski, J. R.; Macchioni, A.; Clot, E.; Eisenstein, O.; Crabtree, R. H. *J. Am. Chem. Soc.* **2005**, *127*, 16299−16311.
(2) Martins, A. M.; Ascenso, J. R.; Costa, S. M. B.; Dias, A. R.; Ferreira, H.; Ferreira, J. A. B. *Inorg. Chem.* **2005**, *44*, 9017−9022.
(3) Macchioni, A.; Zuccaccia, C.; Clot, E.; Gruet, K.; Crabtree, R. H. *Organometallics* **2001**, *20*, 2367−2373.
(4) Gruet, K.; Clot, E.; Eisenstein, O.; Lee, D. H.; Patel, B.; Macchioni, A.; Crabtree, R. H. *New J. Chem.* **2003**, *27*, 80−87.
(5) Aullón, G.; Esquius, G.; Lledós, A.; Maseras, F.; Pons, J.; Ros, J. *Organometallics* **2004**, *23*, 5530−5539.
(6) Macchioni, A. *Chem. Rev.* **2005**, *105*, 2039−2073.
(7) Bakhmutova, E. V.; Bakhmutov, V. I.; Belkova, N. V.; Besora, M.; Epstein, L. M.; Lledós, A.; Nikonov, G. I.; Shubina, E. S.; Tomas, J.; Vorontsov, E. V. *Chem.—Eur. J.* **2004**, *10*, 661−671.
(8) Belkova, N. V.; Besora, M.; Epstein, L. M.; Lledós, A.; Maseras, F.; Shubina, E. S. *J. Am. Chem. Soc.* **2003**, *125*, 7715−7725.
(9) Belkova, N. V.; Collange, E.; Dub, P.; Epstein, L. M.; Lemenovskii, D. A.; Lledós, A.; Maresca, O.; Maseras, F.; Poli, R.; Revin, P. O.; Shubina, E. S.; Vorontsov, E. V. *Chem.—Eur. J.* **2005**, *11*, 873−888.
(10) Belkova, N. V.; Revin, P. O.; Epstein, L. M.; Vorontsov, E. V.; Bakhmutov, V. I.; Shubina, E. S.; Collange, E.; Poli, R. *J. Am. Chem. Soc.* **2003**, *125*, 11106−11115.
(11) Basallote, M. G.; Duran, J.; Fernández-Trujillo, M. J.; Máñez, M. A. *J. Chem. Soc., Dalton Trans.* **1998**, 2205−2210.
(12) Morris, R. H. In *Recent Advances in Hydride Chemistry*; Poli, R., Ed.; Elsevier: Amsterdam, 2001.
(13) Belkova, N. V.; Ionidis, A. V.; Epstein, L. M.; Shubina, E. S.; Gruendemann, S.; Golubev, N. S.; Limbach, H. H. *Eur. J. Inorg. Chem.* **2001**, 1753−1761.
(14) Bakhmutov, V. I. *Eur. J. Inorg. Chem.* **2005**, 245−255.

10.1021/ja070939l CCC: $37.00

Scheme 1. General Representation of Mechanism of Proton Transfer from Proton Donor H−X to Neutral Hydride Complex (Top) and from Coordinated Dihydrogen to Neutral Base B (Bottom)

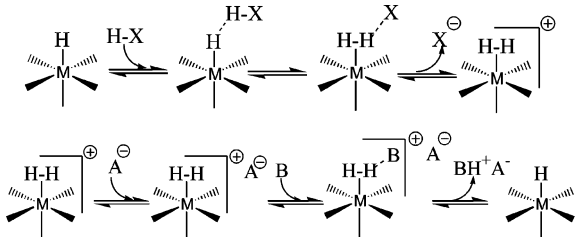

for proton transfer, based on experimental and computational results, is presented in Scheme 1. Proton transfer to the coordinated hydride from an H−X proton donor occurs with the initial formation of an M−H···H−X dihydrogen bond. The reverse process of deprotonation of coordinated H_2 with a neutral base B leads to heterolytic splitting of dihydrogen[15] and is also illustrated in Scheme 1, showing the capability of cationic dihydrogen complexes to allow for the formation of ion pairs with A^- anions.

These ion paired dihydrogen complexes ([M−$H_2^+A^-$]) constitute a remarkable case showing an important effect of the anions on the nature and stability of the intermediates formed in the proton transfer process.[8] The important role of the anion on the stabilization of these species has been shown to be caused by the formation of homoconjugated species of the proton donor (A^- = $ROHOR^-$), which produces more stable [M−(η^2-H_2)]$^+$-[ROHOR]$^-$ ion pairs.[8−9] While in those cases ion pairing of the counterion to the metal complex is responsible for the reactivity changes, there are also some reports showing the consequences of ion pairing with the proton donor on the kinetics of proton transfer. Thus, we have communicated[16] preliminary results showing that the rate of reaction of *trans*-[FeH(η^2-H_2)(dppe)$_2$]$^+$ with NEt_3 is strongly dependent on the nature of the anions in the reaction medium, BF_4^- and PF_6^- causing an acceleration and BPh_4^- a deceleration. Before publication of this study, an investigation on the effect of anions on the selectivity of C−H bond activation was published.[1] The complex $IrH_5(PPh_3)_2$ and 2-pyridylmethyl imidazolium salts yield different kinetic reaction products depending on the nature of the anion (Br^-, BF_4^-, PF_6^-, or SbF_6^-) in the salt, and the authors suggest that the different reactivity in any intermolecular proton transfer could be explained by the different capability of the anions to follow the migrating proton. Gusev has also shown recently the utility of DFT studies to demonstrate that the H−H distance in dihydrogen complexes can be very sensitive to intra- and intermolecular interactions, including ion pairing.[17] More recently, the effect of ion pairing with BF_4^- has been analyzed for the reaction of the hydride cluster $[W_3S_4H_3(dmpe)_3]^+$ with HCl, kinetic and theoretical results showing that in this case the formation of ($[W_3S_4H_3(dmpe)_3]^+$, BF_4^-) ion pairs and the interaction of the anion with the acid lead to a decrease in the rate of reaction.[18]

Dihydrogen bonding and ion pairing are two types of processes involving relatively weak noncovalent interactions. In those cases where both processes are possible, they can behave either in a cooperative way, facilitating the formation of reaction products for thermodynamic and/or kinetic reasons, or in a competitive way that can lead to a partial or complete blockage of the reaction. The effect of anions in proton transfers involving the *trans*-[FeH(η^2-H_2)(dppe)$_2$]$^+$ and $[W_3S_4H_3(dmpe)_3]^+$ complexes illustrates both possibilities. Thus, it is evident that a precise understanding of the thermodynamic and kinetic effects associated to ion pairing would be of great help for tuning the reactivity of hydride and dihydrogen complexes. In this sense, we now describe more detailed experimental and theoretical investigations on the effect of anions on the reaction of *trans*-[FeH(η^2-H_2)(dppe)$_2$]$^+$ (**1**$^+$) with triethylamine according to eq 1.

$$\textit{trans}\text{-}[FeH(H_2)(dppe)_2]^+ + NEt_3 \rightarrow \textit{cis}\text{-}[FeH_2(dppe)_2] + HNEt_3^+ \quad (1)$$

Complex **1**$^+$ was initially prepared by Morris and co-workers as the BF_4^- salt,[19] and studies since then have provided very interesting information on its structure, spectral properties, intramolecular H/H_2 exchange, acidity, and reactivity of the coordinated dihydrogen.[11,20−24] As previously described, the reaction in eq 1 occurs with proton transfer and isomerization, yielding *cis*-[FeH_2(dppe)$_2$] (**2**) and the protonated amine $HNEt_3^+$.[16] Kinetic measurements in THF and acetone solutions indicate that the reaction pathway through the free metal complex is less efficient than that through ion pairs with the BF_4^- and PF_6^- anions. In contrast, ion pairing with BPh_4^- leads to a dead-end in the reaction mechanism. The equilibrium constants for the formation of ion pairs and rate constants for their conversion to final products can be resolved in acetone solution, thus providing quantitative indicators for the thermodynamic and kinetic effects caused by anions. Detailed theoretical calculations provide complementary information about the structure of the ion pairs and their role in the reaction mechanism.

Results and Discussion

Kinetic Studies on the Effect of Ion Pairing to External Anions on the Proton Transfer from *trans*-[FeH(H_2)(dppe)$_2$]$^+$ to NEt_3. In the present work, we have carried out more detailed kinetic studies both in THF and in acetone solution to obtain more information about the role of ion pairs on the stability and kinetics of proton transfer from the dihydrogen complex *trans*-[FeH(H_2)(dppe)$_2$]$^+$ (**1**$^+$). In the presence of a large excess of base, the reaction of **1**$^+$ with NEt_3 occurs according to eq 1 both in THF and in acetone solution. Despite the wrong order of pK_a values for the proton transfer (12 for **1**$^+$ and 10.7 for $HNEt_3^+$ in an aqueous scale[22] and 13 for **1**$^+$ and 12.5 for $HNEt_3^+$ in a THF scale[24]), the values are sufficiently close to allow the reaction to be forced to completion by adding a large

(15) Kubas, G. J. *Adv. Inorg. Chem.* **2004**, *56*, 127−177.
(16) Basallote, M. G.; Besora, M.; Duran, J.; Fernández-Trujillo, M. J.; Lledós, A.; Máñez, M. A.; Maseras, F. *J. Am. Chem. Soc.* **2004**, *126*, 2320−2321.
(17) Gusev, D. G. *J. Am. Chem. Soc.* **2004**, *126*, 14249−14257.
(18) Algarra, A. S. G.; Basallote, M. G.; Fernández-Trujillo, M. J.; Llusar, R.; Safont, V. S.; Vicent, C. *Inorg. Chem.* **2006**, *45*, 5774−5784.
(19) Morris, R. H.; Sawyer, J. F.; Shiralian, M.; Zubkowski, J. D. *J. Am. Chem. Soc.* **1985**, *107*, 5581−5582.
(20) Jia, G.; Morris, R. H. *Inorg. Chem.* **1990**, *29*, 581−582.
(21) Bautista, M.; Earl, K. A.; Morris, R. H.; Sella, A. *J. Am. Chem. Soc.* **1987**, *109*, 3780−3782.
(22) Cappellani, E. P.; Drouin, S. D.; Jia, G.; Maltby, P. A.; Morris, R. H.; Schweitzer, C. T. *J. Am. Chem. Soc.* **1994**, *116*, 3375−3388.
(23) Basallote, M. G.; Durán, J.; Fernández-Trujillo, M. J.; González, G.; Máñez, M. A.; Martínez, M. *Inorg. Chem.* **1998**, *37*, 1623−1628.
(24) Abdur-Rashid, K.; Fong, T. P.; Greaves, B.; Gusev, D. G.; Hinman, J. G.; Landau, S. E.; Lough, A. J.; Morris, R. H. *J. Am. Chem. Soc.* **2000**, *122*, 9155−9171.

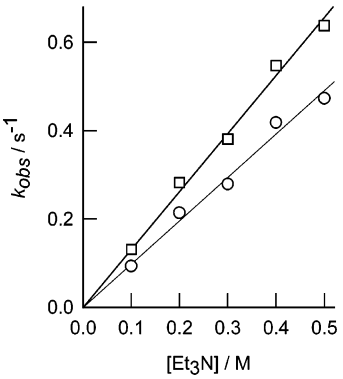

Figure 1. Plots showing the dependence with the concentration of added base of the observed rate constant for the reaction of *trans*-[$FeH(H_2)(dppe)_2$]-(BF_4) (1.0×10^{-3} M) with NEt_3 in THF (circles) or acetone (squares) solution at 25.0 °C in the absence of added salts.

excess of base, as shown by NMR experiments. In the absence of any added salt, kinetic experiments in THF solution using the stopped-flow technique confirmed previous results in the sense that the proton transfer process occurs in a single step with observed rate constants that change linearly with the base concentration (eq 2; see Figure 1). The value derived for the second-order rate constant k at 25.0 °C obtained in the present work (0.98 ± 0.03 M^{-1} s^{-1}) is in reasonable agreement with the previously reported one (0.19 M^{-1} s^{-1}). Although the difference is somewhat larger than usual, it can be understood by considering the difficulties associated to kinetic measurements using air- and water-sensitive compounds, the different samples of reagents used in both kinetic studies, and some changes made in the hardware of the stopped-flow instrument between both sets of experiments.

When the kinetic experiments are carried out in the presence of an excess of Bu_4NBF_4, the rate law is maintained, but the proton transfer is accelerated ($k_{BF_4} = 5.20 \pm 0.02$ M^{-1} s^{-1}) by a factor of 5.3, whereas the acceleration caused by an excess of Bu_4NPF_6 is significantly smaller ($k_{PF_6} = 1.26 \pm 0.07$ M^{-1} s^{-1}, $k_{PF_6}/k = 1.3$). These results are also in reasonable agreement with those previously reported (accelerating factors of 9.3 and 1.5 for BF_4^- and PF_6^-, respectively). It is also interesting to note that the values of the second-order rate constants in THF solution and in the presence of added salts are not affected by further increases of the salt concentration. Although in our previous study we were unable to obtain reliable kinetic measurements in the presence of added $NaBPh_4$ and only a qualitative indication of a decelerating effect of this anion could be obtained, in the present work, a value of 0.68 M^{-1} s^{-1} could be measured in the presence of this salt (2×10^{-3} M), thus confirming the previous qualitative observation. Unfortunately, reliable kinetic results could not be obtained at higher concentrations of $NaBPh_4$ for solubility reasons. Changing the added salt to Bu_4NBPh_4 did not lead to better results; although the reaction clearly occurs more slowly, the kinetic traces are not well-behaved, and no satisfactory fit could be obtained. Some attempts to make kinetic studies using the BPh_4^- salt of the complex also lead to very slow spectral changes, in agreement with the results derived from studies with the BF_4^- salt. However, the reaction becomes so slow that the kinetic data are not reliable, probably because of oxidation problems.

$$k_{obs} = k[NEt_3] \tag{2}$$

As the proton transfer in eq 1 involves the reaction of a cation with a neutral molecule, the effects of ionic strength on the rate constant are expected to be small and similar for all three salts, the different behavior observed for the three anions being indicative of their participation in the reaction mechanism through the formation of ion pairs with a different reactivity. Thus, these kinetic data in THF solution can be rationalized by considering that $\mathbf{1}^+$ forms ion pairs with the X^- anions ($X = BF_4$, PF_6) and that these ion pairs are deprotonated with second-order rate constants k_X significantly different from that corresponding to deprotonation of unpaired $\mathbf{1}^+$ (k_0). This mechanism is depicted in eqs 3−5, and consideration of the ion pairing process (eq 3) as a rapid pre-equilibrium followed by rate-determining conversion to products through two parallel pathways (eqs 4 and 5) leads to the rate law in eq 6. The independence of the experimental rate constant values with respect to the concentration of added salt would be indicative of complete conversion to the ion pair ($1 \ll K_{ipX}[X^-]$) when an excess of X^- is added in THF solution, so that only the values of k_X for the ion pairs with the different anions can be measured. Nevertheless, as the solutions used in the kinetic studies always contain the counteranion present in the solid complex (BF_4^- in this case), determination of the rate constant for deprotonation of the unpaired complex (k_0) is not possible with the present data because a precise separation of the contributions corresponding to both pathways requires the observation of a dependence of the type given by eq 6. The deceleration observed when $X^- = BPh_4^-$ can be explained by considering formation of ($\mathbf{1}^+$, BPh_4^-) ion pairs unable to evolve to the final reaction product, so that the reaction can only proceed through unpaired $\mathbf{1}^+$ or through the ($\mathbf{1}^+$, BF_4^-) ion pairs formed with the BF_4^- anions existing as counteranions in the complex sample.

$$\mathbf{1}^+ + X^- \rightleftarrows (\mathbf{1}^+, X^-);\ K_{ipX} \tag{3}$$

$$\mathbf{1}^+ + Et_3N \rightarrow \textit{cis}\text{-}[FeH_2(dppe)_2] + Et_3NH^+;\ k_0 \tag{4}$$

$$(\mathbf{1}^+, X^-) + Et_3N \rightarrow \textit{cis}\text{-}[FeH_2(dppe)_2] + (Et_3NH^+, X^-);\ k_X \tag{5}$$

$$k_{obs} = \frac{k_0 + k_X K_{ipX}[X^-]}{1 + K_{ipX}[X^-]}[Et_3N] \tag{6}$$

To obtain more information about the effect of added salts and ion pairing on the kinetics of the reaction in eq 1, stopped-flow experiments were also carried out in acetone solution. The dielectric constant of acetone (20.7) is significantly higher than that of THF (7.6), so that the formation of ion pairs is now expected to be less favored. Kinetic data in the absence of added salt are quite similar for both solvents (see Figure 1), and the value derived for k in acetone solution is 1.31 ± 0.02 M^{-1} s^{-1}. However, the rate constants obtained in the presence of added salts now show a clear dependence with respect to the salt concentration. This dependence is illustrated in Figure 2, which shows typical saturation curves for the change of the second-order rate constant k with the concentration of the different salts, BF_4^- and PF_6^- showing again acceleration and BPh_4^- deceleration. For solubility reasons, only the Na^+ salt of BPh_4^- could be used in the acetone solution. As all the kinetic experiments were carried out with solutions prepared from a sample of solid

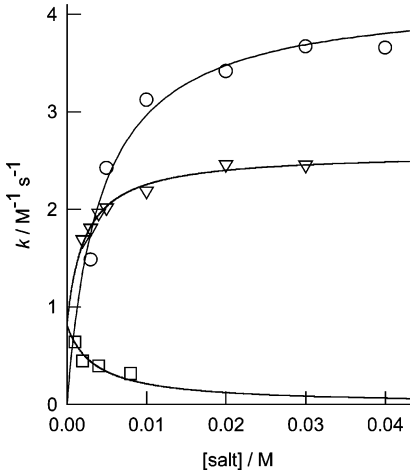

Figure 2. Plots showing the dependence with the concentration of added salt of the second-order constant for the reaction of *trans*-[FeH(H_2)(dppe)$_2$]$^+$ (**1**$^+$, 1.0×10^{-3} M) with NEt_3 in acetone solution at 25.0 °C. The circles correspond to data in the presence of added Bu_4NBF_4, the triangles to Bu_4NPF_6, and the squares to $NaBPh_4$. The solid lines represent the best fits of the data to the equations indicated in the text. Note that the plots corresponding to Bu_4NPF_6 and $NaBPh_4$ have nonzero intercepts because of the contribution of the (**1**$^+$, BF_4^-) ion pairs formed with the counteranion of the complex sample.

trans-[FeH(H_2)(dppe)$_2$]BF_4, the BF_4^- anion is always present, and its effect must be considered when analyzing the kinetic data in the presence of other anions. Figure 2 shows that the values of k increase with the BF_4^- concentration according to saturation kinetics to reach a limiting value somewhat higher than 4 M^{-1} s^{-1}. Actually, a satisfactory fit of the data by eq 6 can be obtained with $k_{BF_4} = 4.2 \pm 0.2$ M^{-1} s^{-1}, $K_{ipBF_4} = (2.4 \pm 0.4) \times 10^2$ M^{-1}, and a negligible value of k_0, which indicates that the reaction can be considered to go exclusively through the ion pair pathway (eqs 3 and 5). The lower dielectric constant of THF anticipates a higher stability of the ion pair (higher value of K_{ipBF_4}), so that the k_0 pathway would also be negligible in that solvent and that the rate constants measured in the absence of added salt in both solvents would then correspond to the contribution of ion pairs formed with the BF_4^- counteranion in the complex sample. Moreover, the close values obtained for the rate constants for proton transfer from the (**1**$^+$, BF_4^-) ion pair to the base (k_{BF_4} values of 5.2 and 4.2 M^{-1} s^{-1} in THF and acetone, respectively) reveal that, once the ion pair is formed, the rate of reaction with NEt_3 is essentially independent of the solvent nature.

When the reaction is carried out in the presence of added Bu_4NPF_6, the reaction can go through two parallel pathways involving the (**1**$^+$, BF_4^-) and (**1**$^+$, PF_6^-) ion pairs, and eqs 7 and 8 must be added to the mechanistic proposal to account for the contribution of both types of ion pairs to the net rate of reaction. In this case, the derivation of the rate law requires consideration of two rapid pre-equilibria (eqs 3 and 7) and three parallel rate-determining pathways for conversion to products (eqs 4, 5, and 8). Under those considerations, the rate law is given by eq 9, specifically for $X^- = BF_4^-$ and $Y^- = PF_6^-$, which allows a satisfactory fit of the experimental data in the presence of added Bu_4NPF_6 by fixing k_{BF_4} and K_{ipBF_4} at the values previously determined. In this way, values of $k_{PF_6} = 2.58 \pm 0.04$ M^{-1} s^{-1} and $K_{ipPF_6} = (5.5 \pm 0.5) \times 10^2$ M^{-1} are obtained. Again, the value of k_{PF_6} in acetone solution is smaller than k_{BF_4} and compares well with the value determined in THF. On the other hand, K_{ipPF_6} is only slightly higher than K_{ipBF_4}, which indicates that both anions are able to form quite stable ion pairs with **1**$^+$ under the experimental conditions used. As a summary, it can be stated that PF_6^- forms more stable ion pairs than those formed by BF_4^-, although they are less efficient for accelerating the deprotonation process. Nevertheless, it must also be pointed out that k_{BF_4} and k_{PF_6} are of the same order of magnitude and that both types of ion pairs provide a reaction pathway much faster than that operating for the unpaired metal complex. The k_{BF_4}/k_{PF_6} quotients of 4.1 in THF and 1.6 in acetone indicate that the difference between the rates of deprotonation through the BF_4^- and PF_6^- ion pairs is somewhat reduced in acetone solution.

$$\mathbf{1}^+ + Y^- \rightleftarrows (\mathbf{1}^+, Y^-);\ K_{ipY} \qquad (7)$$

$$(\mathbf{1}^+, Y^-) + Et_3N \rightarrow cis\text{-}[FeH_2(dppe)_2] + (Et_3NH^+, X^-);\ k_Y \qquad (8)$$

$$k_{obs} = \frac{k_0 + k_X K_{ipX}[X^-] + k_Y K_{ipY}[Y^-]}{1 + K_{ipX}[X^-] + K_{ipY}[Y^-]} \qquad (9)$$

The data in the presence of added $NaBPh_4$ can be fitted using the same procedure, although considering that the (**1**$^+$, BPh_4^-) ion pairs are unable to evolve to the reaction products (k_{BPh_4} is negligible). In that case, the fit only leads to a value of $K_{ipBPh_4} = (3.5 \pm 0.6) \times 10^2$ M^{-1}, which indicates that BPh_4^- forms ion pairs with a stability similar to that of those formed with the BF_4^- and PF_6^- anions, although they are unproductive for proton transfer.

Computational Studies. Although the kinetic data clearly indicate an important effect of the external anions on the kinetics of proton transfer from complex **1**$^+$, they do not provide any information about the reasons leading to an acceleration or deceleration of the reaction. For this reason, theoretical calculations were carried out both in the absence and in the presence of the BF_4^-, PF_6^-, and BPh_4^- anions. To simplify the calculations, the model complex *trans*-[FeH(η^2-H_2)(dhpe)$_2$]$^+$ (dhpe = $H_2P-CH_2CH_2-PH_2$), where the phenyl groups of the dppe ligand have been substituted by hydrogen atoms, and the base NMe_3 were used.

Order of Occurrence of the Isomerization and Proton Transfer Processes. As deprotonation of *trans*-[FeH(η^2-H_2)(dppe)$_2$]$^+$ by triethylamine leads to the formation of *cis*-[FeH_2(dppe)$_2$], the proton transfer is accompanied by an isomerization step, which can precede or follow the proton transfer. Unfortunately, the reaction occurs in a single kinetic step, and so kinetic studies do not provide information about this point. In a previous work on the kinetics of reaction of *cis*-[FeH_2(dppe)$_2$] with acids,[11] it was proposed on the basis of comparative data with the related *cis*-[$FeH_2(PP_3)$] complex ($PP_3 = P(CH_2CH_2PPh_2)_3$) that the proton transfer occurs between the trans forms of both complexes. However, Morris and co-workers had suggested that the deprotonation of *trans*-[FeH(H_2)(dppe)$_2$]$^+$ occurs with the initial formation of the *trans*-dihydride, which was actually observed in low-temperature experiments of deprotonation of the related Ru and Os complexes.[22] Later work on the protonation of *cis*-[RuH_2(dppe)$_2$] with acids revealed that the trans isomer reacts much faster than the cis form, so that

Scheme 2. Alternative Reaction Pathways for Reaction of *trans*-**1**$^+$ with Base to Yield *cis*-Dihydride **2**[a]

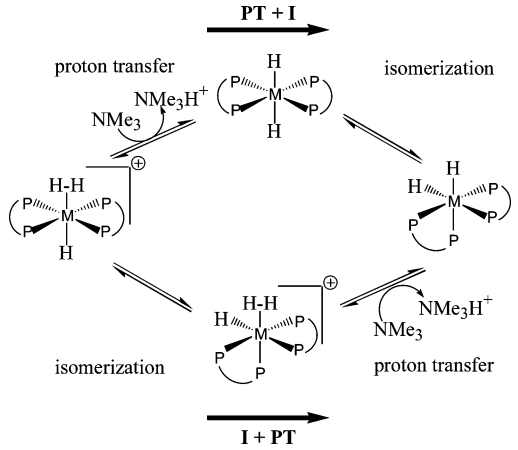

[a] Both pathways differ in order of occurrence of proton transfer (**PT**) and isomerization (**I**) processes: **PT** + **I** (upper pathway) and **I** + **PT** (lower pathway).

Table 1. Relative Energies of Different Species Involved in Isomerization Processes (kcal/mol)

species	gas phase	THF	acetone
	[FeH(η^2-H$_2$)(dhpe)$_2$]$^+$ Isomerization		
trans-H$_2$	0.0	0.0	0.0
TS[H$_2$]	31.7	31.9	32.2
cis-H$_2$	2.8	2.4	2.4
	[FeH$_2$(dhpe)$_2$] Isomerization		
trans-H	0.0	0.0	0.0
TS[H]	16.7	17.9	19.3
cis-H	−5.1	−4.6	−4.6

the kinetic data for the reactions of both Ru and Fe complexes can be interpreted by considering that these reactions occur through initial isomerization followed by reaction with the acid,[25] in agreement with the proposal by Morris and co-workers.[22] Nevertheless, as the present study was carried out in the deprotonation direction and using a reagent different from those used in previous protonation studies, it was considered of fundamental concern to carry out theoretical calculations aimed at determining the order in which the proton transfer and isomerization processes occur. The two possibilities are represented in Scheme 2, where the **PT** + **I** pathway corresponds to proton transfer from *trans*-[FeH(η^2-H$_2$)(dppe)$_2$]$^+$ to form *trans*-[FeH$_2$(dppe)$_2$] followed by isomerization and the **I** + **PT** pathway corresponds to initial isomerization to *cis*-[FeH(η^2-H$_2$)(dppe)$_2$]$^+$ followed by proton transfer.

To decide which process occurs first, the isomerization step was theoretically studied both for *trans*-[FeH$_2$(dhpe)$_2$] (eq 10) and for *trans*-[FeH(η^2-H$_2$)(dhpe)$_2$]$^+$ (eq 11).

$$\textit{trans}\text{-}[\mathrm{FeH_2(dhpe)_2}] \rightleftarrows \textit{cis}\text{-}[\mathrm{FeH_2(dhpe)_2}] \qquad (10)$$

$$\textit{trans}\text{-}[\mathrm{FeH}(\eta^2\text{-}\mathrm{H_2})(\mathrm{dhpe})_2]^+ \rightleftarrows \textit{cis}\text{-}[\mathrm{FeH}(\eta^2\text{-}\mathrm{H_2})(\mathrm{dhpe})_2]^+ \qquad (11)$$

The relative energies of all the species involved in both isomerization processes in the gas phase and THF and acetone solvents are collected in Table 1. In the gas phase, the calculations for the isomerization of the dihydride complex, eq 10, show that the cis product is 5.1 kcal/mol more stable than the *trans*-dihydride, whereas for the hydride−dihydrogen complex, eq 11, the *cis*-hydride−dihydrogen product is 2.8 kcal/mol less stable than the *trans*-hydride−dihydrogen complex. These results are in agreement with the experimental observations, which indicate that the trans isomer is favored for the starting complex, while the reaction product exists as the cis isomer. However, to determine which one of the pathways in Scheme 2 is preferred, it is necessary to also know the barriers for these isomerizations, and so the corresponding transition states (**TS[H$_2$]** and **TS[H]**) were also located.

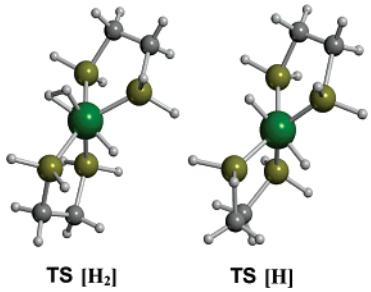

Figure 3. Geometries of the transition states calculated for isomerization of *trans*-[FeH(η^2-H$_2$)(dhpe)$_2$]$^+$ and *trans*-[FeH$_2$(dhpe)$_2$]. They correspond to the isomerization processes occurring in the **I** + **PT** and **PT** + **I** pathways in Scheme 2.

In the gas phase, the transition state for isomerization of the *trans*-dihydride complex was found to be 16.7 kcal/mol above the energy of the *trans*-dihydride. Its geometry, labeled as **TS-[H]** in Figure 3, shows that the coordination around the metal center can be described as a trigonal prism with ligands at each vertex, which corresponds to a 60° rotation of three ligands in the starting octahedral complex. On the other hand, the transition state for isomerization of the *trans*-hydride−dihydrogen complex is placed 31.7 kcal/mol above the energy of the trans isomer. This species is labeled as **TS[H$_2$]** in Figure 3, and it also shows a hexacoordinated trigonal prism geometry with one of the vertices occupied by the dihydrogen ligand. Solvent effects in the isomerization processes are small. The smaller difference between both energy barriers is found in acetone, being that the activation barrier for the dihydride isomerization is 12.9 kcal/mol lower than that for dihydrogen isomerization. Thus, theoretical calculations indicate that the isomerization barriers are significantly different for the *trans*-dihydride and the dihydrogen complexes, favoring the **PT** + **I** ordering in Scheme 2. This conclusion is in agreement with the previous proposal of Morris and co-workers,[22] and the calculations on the proton transfer process were then carried out considering that this process occurs in the starting complex and that isomerization to the final product occurs in the final step.

Theoretical Studies on the Deprotonation Mechanism. Computational investigations on the deprotonation of *trans*-[FeH(η^2-H$_2$)(dhpe)$_2$]$^+$ (**1t**) were first carried out without considering any anion. With this simplification, the system does not correspond exactly to any experimental case because at least the BF_4^- counteranions are present in solution. However, these calculations were required to obtain information about the way in which proton transfer would occur through the unpaired dihydrogen complex (k_0 pathway, eq 4). Although kinetic data indicate that the contribution of this pathway is negligible both in THF and in acetone solutions, knowledge of the nature of

(25) Basallote, M. G.; Durán, J.; Fernández-Trujillo, M. J.; Máñez, M. A. *Inorg. Chem.* **1999**, *38*, 5067−5071.

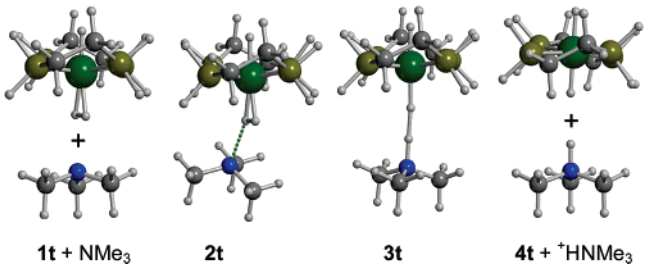

Figure 4. Geometries of the complexes located along the deprotonation of *trans*-[FeH(η^2-H_2)(dhpe)$_2$]$^+$ with NMe_3, without considering the presence of anions.

the processes taking place in the absence of anions is required to compare them with those occurring when the ion pairs are formed.

Calculations in the Absence of Anions. The computational results obtained in the study of the reaction of **1t** with NMe_3 indicate that the reaction goes through a series of intermediate species whose optimized geometries are shown in Figure 4. At this point, it is important to note that the location of several reaction intermediates in the theoretical work is compatible with the experimental observation of a single kinetic step because these intermediates can be considered to be formed under steady-state or rapid pre-equilibria conditions, so that their existence would not be revealed in the kinetic studies.

As a starting point for the calculations, the cationic dihydrogen complex and the base were considered infinitely apart. The *trans*-[FeH(η^2-H_2)(dhpe)$_2$]$^+$ complex shows Fe−H distances of 1.679 Å for the hydrogens of the H_2 ligand and 1.506 Å for the hydride, the H−H distance in the dihydrogen ligand being 0.810 Å. When both species interact, they first form a species *trans*-[FeH(η^2-H_2)(dhpe)$_2$]$^+$···NMe_3 (**2t**) that will be called the interacting complex. In this species, the base approaches the complex at proximities of the H_2 ligand and forces one of the H atoms to separate slightly from the metal center, the Fe−H distances being now 1.734 and 1.676 Å for the dihydrogen ligand and 1.511 Å for the hydride. However, the H−H distance in the H_2 ligand (0.809 Å) does not change upon the formation of **2t**, and the Me_3N−H distances are still quite large (2.443 and 3.047 Å, respectively). These small structural changes indicate the existence of a weak interaction between the nitrogen of the amine and the acidic dihydrogen ligand, as confirmed by the energy values in Table 2. Very recently, experimental evidence that coordinated H_2 can participate in intermolecular hydrogen bonding to H-bond acceptors has been given.[26]

The interacting complex **2t** evolves to a species *trans*-[(dhpe)$_2$HFeH···H···NMe_3]$^+$ (**3t**) that can be described as a dihydrogen bonded adduct, in which the proton transfer has already occurred to a significant extent. The energy changes associated to this transformation are also small, species **3t** being only 4.8 kcal/mol more stable than the reactants in the gas phase and slightly less stable in THF or acetone solution (see Table 2). The dihydrogen bonded species **3t** shows a quite unusual geometry. The H−H distance it exhibits (1.211 Å) is short enough to consider this species as containing an elongated dihydrogen ligand coordinated in an end-on way.[27−29] The

Table 2. Calculated Energies (kcal/mol) for Different Species Involved in Deprotonation Process of *trans*-[FeH(H_2)(dhpe)$_2$]$^+$ (**1t**) with NMe_3 to Form *cis*-[FeH_2(dhpe)$_2$] (**5t**)[a]

species	gas phase	THF	acetone
Unpaired metal complex			
1t + NMe_3	0	0	0
2t	−5.4	2.5	2.4
3t	−4.8	3.0	2.6
4t + $HNMe_3^+$	25.6	11.5	10.0
5t + $HNMe_3^+$	20.5	6.9	5.4
BF_4^- ion pairs			
1t + NMe_3 + BF_4^-	0	0	0
(**1t**, BF_4^-) + NMe_3	−85.5	−15.8	−9.4
2t-BF_4^-	−92.9	−14.9	−8.9
3t-BF_4^-	−92.5	−15.0	−9.4
3b-BF_4^-	−94.5	−14.6	−11.1
4t + ($HNMe_3^+$, BF_4^-)	−84.6	−15.8	−7.6
5t + ($HNMe_3^+$, BF_4^-)	−89.7	−20.4	−12.2
PF_6^- ion pairs			
1t + NMe_3 + PF_6^-	0	0	0
(**1t**, PF_6^-) + NMe_3	−80.5	−17.5	−11.3
2t-PF_6^-	−89.2	−17.7	−12.3
3t-PF_6^-	−88.1	−15.9	−10.2
3b-PF_6^-	−89.4	−16.1	−10.5
4t + ($HNMe_3^+$, PF_6^-)	−78.2	−14.7	−8.8
5t + ($HNMe_3^+$, PF_6^-)	−83.3	−19.3	−13.5
BPh_4^- ion pairs			
1t + NMe_3 + BPh_4^-	0	0	0
(**1t**, BPh_4^-) + NMe_3	−59.0	1.2	4.0
4t + ($HNMe_3^+$, BPh_4^-)	−56.6	2.8	6.0
5t + ($HNMe_3^+$, BPh_4^-)	−61.6	−1.8	1.4

[a] Table includes results for reaction of unpaired metal complex and for pathways involving ion pairs with different anions.

Fe−H distances are 1.542 Å for the hydride and 1.600 and 2.807 Å for the dihydrogen ligand. The Me_3N−H distance of 1.127 Å is significantly shorter than in **2t** and indicates a substantial degree of N−H bond formation. The Fe(−H)−H−N and N−H−H angles of 178 and 179°, respectively, and the dihedral Fe−H−H−N angle of 175° indicate an almost perfect linear arrangement of the Fe−H−H−N structural subunit.

The reaction coordinate between complexes **2t** and **3t** has been also investigated by making calculations with the optimization of all the parameters except the N−H distance to the transferred proton, which is taken as the reaction coordinate. This distance varies from 2.443 Å in **2t** to 1.127 Å in **3t**. In this way, the energy maximum of the potential energy curve has been located 2.9 kcal/mol above **2t** in the gas phase for a N−H···H−Fe distance of 1.6 Å (Figure 5), which indicates that the activation barrier for the proton transfer is quite small. In THF and acetone, the maximum is located 4.1 and 3.9 kcal/mol above **2t**, respectively. The barriers in solution, although slightly higher than in the gas phase, still agree with a very fast proton transfer step.

In the next step, species **3t** evolves with separation of the products resulting from the proton transfer: *trans*-[FeH_2(dhpe)$_2$] (**4t**) and the protonated amine $HNMe_3^+$. The optimized geometry of **4t** reveals a symmetrical structure with identical Fe−H distances of 1.563 Å. The energy of complex **4t** and the $HNMe_3^+$ cation considered infinitely separated from each other is 25.6 kcal/mol above that of the reactants in the gas phase. Although the solvent decreases the energy cost for the separation of the protonated amine from the dihydride (**4t** + $HNMe_3^+$ are found to be 11.5 and 10.0 kcal/mol above the reactants in the

(26) Szymczak, N. K.; Zakharov, L. N.; Tyler, D. R. *J. Am. Chem. Soc.* **2006**, *128*, 15830−15835.
(27) Osborn, J. A.; Jardine, F. H.; Young, J. F.; Wilkinson, G. *J. Chem. Soc. A* **1966**, 1711−1732.
(28) Vaska, L.; Werneke, M. F. *Ann. N.Y. Acad. Sci.* **1971**, *172*, 546−562.
(29) Heinekey, D. M.; Lledós, A.; Lluch, J. M. *Chem. Soc. Rev.* **2004**, *33*, 175−182.

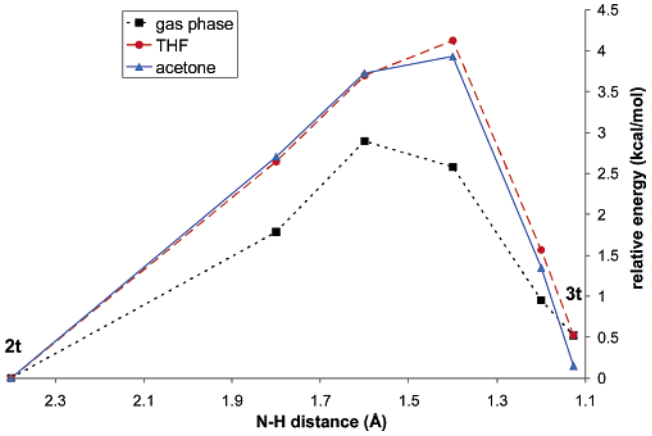

Figure 5. Potential energy curve for the **2t** → **3t** process taking the N−H distance to the transferred proton as the reaction coordinate.

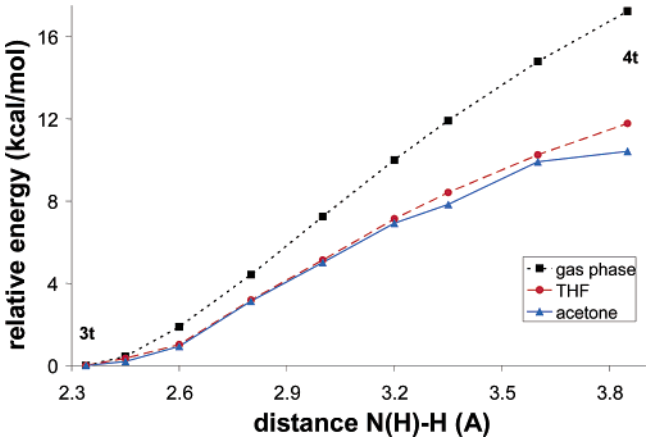

Figure 6. Potential energy curve for the **3t** → **4t** process taking the N···H−Fe distance as the reaction coordinate.

THF and acetone solution, respectively), this is still the most energy-demanding step in the overall proton transfer process. The conversion of complex **3t** to the separated products **4t** and $HNMe_3^+$ has been also investigated taking as a reaction coordinate the distance between the nitrogen atom and the hydride. No maximum was found along the N···H−Fe potential energy curve, the energy increasing monotonically until the separated products both in gas phase and in solution (see Figure 6).

When the proton transfer is completed, the final step consists of isomerization of **4t** to the more stable *cis*-$[FeH_2(dhpe)_2]$ (**5t**), which occurs through the transition state described previously. In the gas phase, the energy of the separated *cis*-dihydride and protonated amine products is 20.5 kcal/mol higher than that of the reactants. Even when the solvent is included, the overall reaction is not favored thermodynamically, in agreement with the pK_a values of both reagents and the experimental observation of the lack of reactivity of the unpaired cation.

Calculations in the Presence of One BF_4^- Anion. The results of theoretical calculations including one BF_4^- anion are of special relevance because this anion is always present at least in a 1:1 molar ratio with respect to the iron complex in the solutions used for the kinetic studies. From the kinetic results, it is expected that a mixture of free and ion paired metal complexes exist in solution, the relative amount of both species depending on the nature of the solvent and the nature and concentration of the anion. Nevertheless, the reaction pathway

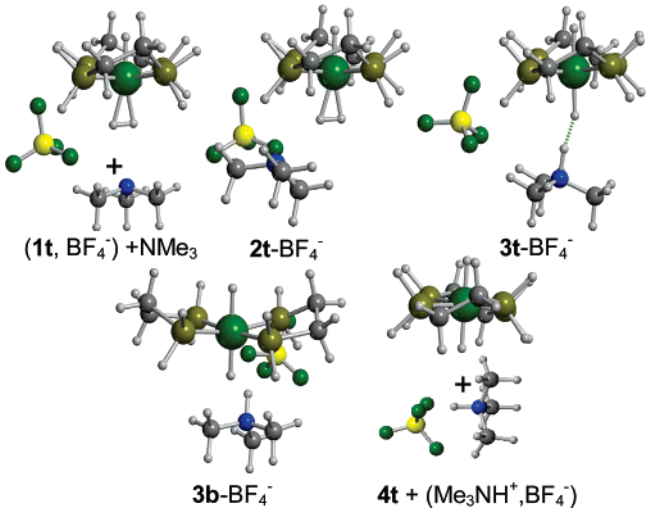

Figure 7. Geometries of the complexes located along the deprotonation of *trans*-$[FeH(\eta^2\text{-}H_2)(dhpe)_2]^+$ with NMe_3 in the presence of a BF_4^- anion.

through the ion paired complex is more efficient, and the reaction goes exclusively through this pathway. Thus, theoretical calculations are expected to provide some information about the reasons leading to this higher efficiency for deprotonation of the ($\mathbf{1}^+$, BF_4^-) ion pairs with respect to free $\mathbf{1}^+$.

As expected, calculations indicate that the formation of an ion pair between *trans*-$[FeH(\eta^2\text{-}H_2)(dhpe)_2]^+$ and BF_4^-, (**1t**, BF_4^-), is favored. Although the stabilization energy is considerably overestimated in the gas phase (85.5 kcal/mol), it is still significant in solution (15.8 and 9.4 kcal/mol in THF and acetone, respectively). Interaction between BF_4^- and NMe_3 leads to significantly smaller values of the stabilization energy (−8.8 in the gas phase, −0.4 in THF, and −0.5 in acetone, all values in kcal/mol). The optimized geometry of the (**1t**, BF_4^-) ion pair (see Figure 7) indicates that BF_4^- approaches the complex at proximities of the coordinated H_2 causing only minor structural changes very similar to those observed for the interaction of **1t** with NMe_3. The Fe−H distances of (**1t**, BF_4^-) are 1.517 Å for the hydride and 1.687 and 1.760 Å for the hydrogen atoms of the H_2 ligand, the H−H distance remaining almost unchanged (0.800 Å). The shorter F−H distance is 2.069 Å, and the preferential interaction of BF_4^- with one of the H atoms results in location of the anion in a space close to two phosphorus atoms of different dhpe ligands, which allows for the approach of the base in the next step. It should be pointed out that the position of the anion is due in part to the modeling of the phosphine. The H−P substituents of the model $H_2P-CH_2-CH_2-PH_2$ ligands are acidic enough to interact with BF_4^-, thus displacing the anion from the H_2 ligand. This interaction is not possible with the actual phenyl substituents.

Actually, calculations indicate that deprotonation can still proceed through a mechanism quite similar to that found in the absence of anions, although the BF_4^- anion participates all along the process. The optimized geometries of the different intermediates are also included in Figure 7. When NMe_3 approaches the (**1t**, BF_4^-) ion pair, the system first evolves to form an interacting complex **2t**-BF_4^-, which is stabilized by −7.4 kcal/mol in the gas phase with respect to the infinitely separated ion pair (**1t**, BF_4^-) and NMe_3 (+0.9 kcal/mol in THF and +0.5 kcal/mol in acetone). Complex **2t**-BF_4^- shows geometrical parameters close to those of (**1t**, BF_4^-); the H−H distance is

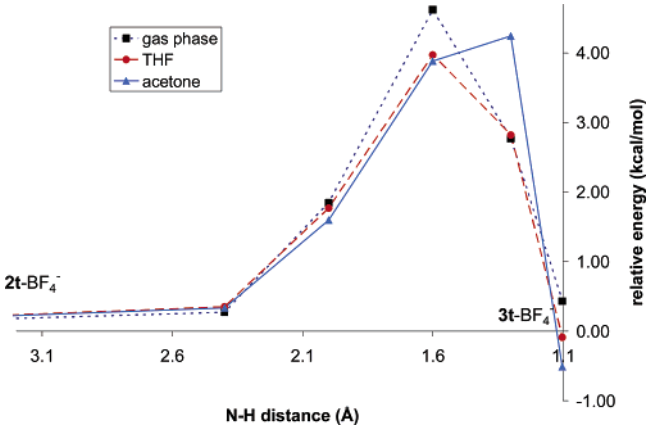

Figure 8. Potential energy curve for the **2t**-BF_4^- → **3t**-BF_4^- process taking the N−H distance of the transferring proton as the reaction coordinate.

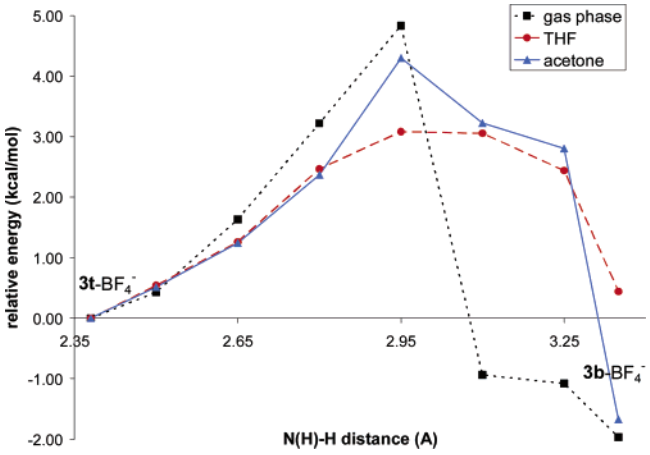

Figure 9. Potential energy curve for the **3t**-BF_4^- → **3b**-BF_4^- process taking the N···H—Fe distance as the reaction coordinate.

maintained at 0.801 Å, and the amine is placed far from the dihydrogen ligand, the Me_3N−H distances of 4.408 and 4.843 Å being significantly larger than in the absence of BF_4^-. Nevertheless, the interacting complex **2t**-BF_4^- undergoes deprotonation through an intermediate species **3t**-BF_4^- that can also be described as containing an elongated dihydrogen ligand coordinated in an end-on way. However, as a consequence of the interaction with the anion, the deviations from the ideal geometry in **3t**-BF_4^- are larger than in **3t**: the Fe−H distances are 1.551, 1.590, and 2.828 Å, the H−H distance is elongated to 1.283 Å, the N−H−H angle is 170°, Fe(H)−H−N is 179°, and the Fe−H−H−N dihedral angle is −179°. The stability associated with the formation of **3t**-BF_4^- is slightly higher than that achieved in **3t**. Whereas **3t** is found 3.0 kcal/mol above **1t** + NMe_3, **3t**-BF_4^- is found only 0.8 kcal/mol above (**1t**, BF_4^-) + NMe_3 (THF values). The potential energy curve from **2t**-BF_4^- to **3t**-BF_4^- has been also investigated by freezing the N−H distance and optimizing the rest of the geometrical parameters (Figure 8). The maximum has been located 4.6 kcal/mol above the **2t**-BF_4^- species in the gas phase for a N−H distance of 1.6 Å (Figure 8). Slightly lower barriers are found in THF (4.0 kcal/mol) and acetone (4.2 kcal/mol). Comparing these values with those reported in Figure 5, it can be appreciated that the presence of the anion practically does not affect the barrier of the proton transfer step in solution, being that this barrier is always quite low.

Complex **3t**-BF_4^- evolves with proton−hydride separation and forms another interacting complex labeled **3b**-BF_4^- in Figure 7. This species is stabilized by −9 kcal/mol in the gas phase with respect to separated (**1t**, BF_4^-) and NMe_3. In solution, it is 1.2 kcal/mol above (THF) and 1.7 kcal/mol below (acetone) the separated (**1t**, BF_4^-) and NMe_3. The Fe−H distances of 1.570 and 1.568 Å, the (Fe)H···H(N) distance of 3.176 Å, and the shorter (N)H···F(B) distance of 1.595 Å indicate that this species can be considered as *trans*-[FeH_2(dhpe)$_2$]-($Me_3NH^+BF_4^-$) (i.e., an ion pair between the protonated amine and the BF_4^- anion, although there is still a weak interaction with the dihydride complex just formed). The reaction coordinate between species **3t**-BF_4^- and **3b**-BF_4^- has been investigated taking the N···H—Fe distance as the reaction coordinate. The maximum of the potential energy curve is found to be 4.8 kcal/mol above complex **3t**-BF_4^- in the gas phase for a N···H distance of 2.95 Å (Figure 9). In solution, the estimated barriers are 3.1 kcal/mol in THF and 4.3 kcal/mol in acetone.

The reaction is completed with conversion of **3b**-BF_4^- to separated **4t** and the (Me_3NH^+, BF_4^-) ion pair, with an energy 0.9 kcal/mol above separated (**1t**, BF_4^-) and NMe_3 in the gas phase (0.0 and 1.8 kcal/mol in THF and acetone, respectively). The small energy changes associated with this step are consistent with the small structural changes involved (i.e., the breaking of the weak interaction between **4t** and the ion pair). Complex **4t** then isomerizes to the more stable *cis*-dihydride **5t**, in such a way that the reaction products for the overall deprotonation process are located 4.2 kcal/mol under the reactants, (**1t**, BF_4^-) and the amine, in the gas phase (4.6 and 2.8 kcal/mol in THF and acetone, respectively). These values are significantly different from those observed for the reaction of the unpaired **1t** complex and indicate that deprotonation of the ion pair is more favored thermodynamically than the same reaction for the free metal complex. In addition to this thermodynamic effect, ion pairing with BF_4^- also decreases the barrier associated with the conversion of **3t**-BF_4^- to **4t** + (Me_3NH^+, BF_4^-). Without the anion, the energy increases monotonically from **3t** to **4t** + Me_3NH^+ (Figure 6), and the required energies for the separation process are 30.4 kcal/mol (gas phase), 8.5 kcal/mol (THF), and 7.4 kcal/mol (acetone) (see Table 2). When the anion is present, the highest barrier for the overall **3t**-BF_4^- → **4t** + (Me_3NH^+, BF_4^-) process is 7.9 kcal/ mol in the gas phase and 3.1 and 4.3 kcal/mol in THF and acetone, respectively. Comparing the energy values without and with the anion, it is obtained that the **3t**-BF_4^- → **4t** + (Me_3NH^+, BF_4^-) separation requires 22.5 kcal/mol less energy than the conversion of **3t** in **4t** + Me_3NH^+ in the gas phase and 5.4 and 3.1 kcal/mol in THF and acetone solution, respectively. As the energy required for achieving the **4t** + ($HNMe_3^+$, BF_4^-) state from (**1t**, BF_4^-) + NMe_3 is lower than that required for achieving **4t** + $HNMe_3^+$ in the pathway going through unpaired **1t**, the overall activation barrier for conversion of **1t** to **5t** is significantly smaller through the BF_4^- ion pairs. Moreover, as the barriers for the proton transfer process are rather small in the presence of the anion, it can be considered that the reaction goes through a rapid pre-equilibrium of conversion of (**1t**, BF_4^-) + NMe_3 to **4t** + (Me_3NH^+, BF_4^-) followed by rate-determining isomerization of the dihydride. The activation barrier would thus correspond to the isomerization step, although the rate of the overall reaction would change linearly with the amount of **4t** formed in the equilibrium. As the energies associated with the proton transfer

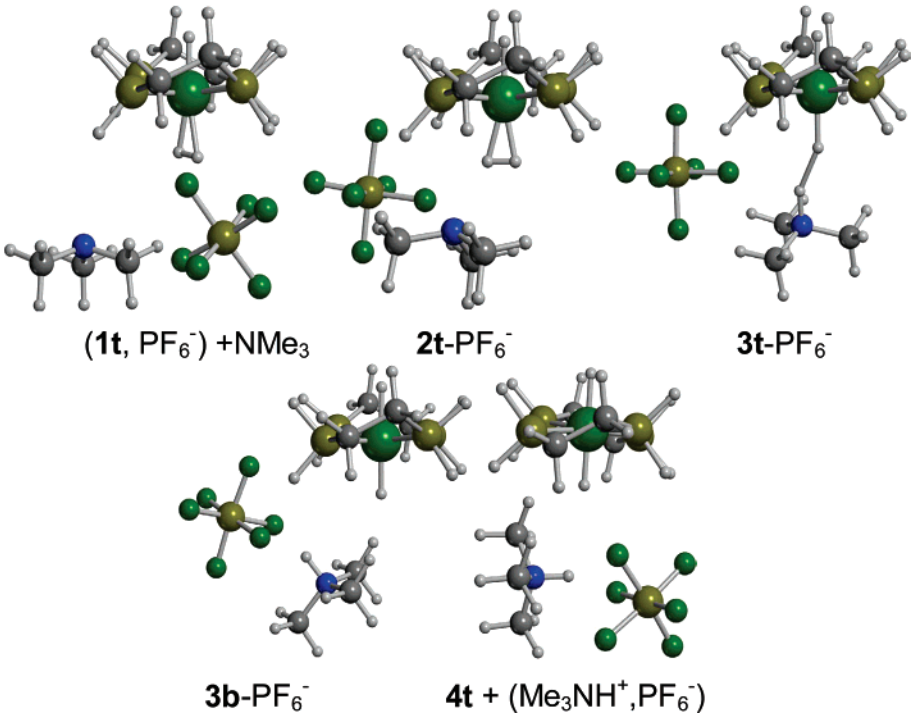

Figure 10. Geometries of the complexes located along the *trans*-[FeH(η^2-H_2)(dhpe)$_2$]$^+$ deprotonation with NMe_3 in the presence of a PF_6^- anion.

pre-equilibrium are 0.0 and 1.8 kcal/mol in THF and acetone, respectively, the degree of conversion to **4t** will be somewhat lower in acetone, thus justifying the lower efficiency of the ion pairing pathway in this solvent. As a summary, these theoretical results explain the acceleration observed in the kinetic studies and indicate that the major role of BF_4^- would be to provide a reaction pathway through ion pairs that involves a lower barrier for the proton transfer and that leads to more stable reaction products, these effects being caused mainly by the capability of BF_4^- to assist the proton transfer and the separation of the resulting products.

Calculations in the Presence of the PF_6^- and BPh_4^- Anions. According to the kinetic results, the formation of ion pairs with the PF_6^- anion causes an acceleration of the deprotonation process similar to that achieved with BF_4^-, although the rate of reaction is somewhat smaller for the case of PF_6^-. To shed some light on the different reaction rates observed for the ion pairs with both anions, theoretical calculations on the deprotonation process were also carried out including one PF_6^- anion. The results summarized in Table 2 indicate that the formation of the ion pair between dihydrogen complex and PF_6^- is favored by 80.5 kcal/mol in the gas phase and by 17.5 and 11.3 kcal/mol in THF and acetone, respectively. Comparing the stabilization energies of the (**1t**, BF_4^-) and (**1t**, PF_6^-) ion pairs, a slightly higher value is obtained for the PF_6^- ion pair, both in THF and in acetone (Table 2). This result agrees with the slightly higher stability of the PF_6^- ion pair deduced from the K_{ipBF_4} and K_{ipPF_6} values derived from the kinetic data. The geometrical parameters of the (**1t**, PF_6^-) ion pair are quite similar to those of (**1t**, BF_4), the Fe−H distances being now 1.517, 1.675, and 1.747 Å and the H−H distance 0.798 Å.

From the (**1t**, PF_6^-) ion pair, deprotonation can go through a pathway quite similar to that described previously for the BF_4^- anion. The optimized geometries of the different species are shown in Figure 10, and the energy values are in Table 2. As for BF_4^-, the reaction pathway going through the PF_6^- ion pairs is slightly favored thermodynamically, in contrast to the results for the unpaired metal complex. The activation barrier for the proton transfer process is also drastically reduced in the presence of this anion, so that the overall process can also be considered to occur through a rapid proton transfer pre-equilibrium followed by rate-determining isomerization. It is also interesting to note that the equilibrium of conversion of (**1t**, PF_6^-) + NMe_3 to **4t** + ($HNMe_3^+$, PF_6^-) (calculated energies of 2.8 and 2.5 kcal/mol in THF and acetone, respectively) is less favored than for the BF_4^- ion pairs. As the activation barrier for isomerization is the same in both cases, this justifies the lower efficiency of the PF_6^- ion pairs with respect to their BF_4^- analogues. Moreover, the larger experimental k_{PF_6} value in acetone solution can be associated with the fact that the energy difference between the **4t** + ($HNMe_3^+$, PF_6^-) and (**1t**, PF_6^-) + NMe_3 states is smaller in acetone than in THF, in contrast to the BF_4^- anion for which both the experimental and the theoretical results indicate a faster reaction in THF.

In contrast to BF_4^- and PF_6^-, the ion pairs formed with the BPh_4^- anion do not provide a reaction pathway productive for the proton transfer process, which results in a decrease in the observed rate of reaction. The calculations in the presence of this anion show two interesting features of the ion pair formed between **1t** and BPh_4^-. The first one is that the (**1t**, BPh_4^-) ion pair is less stabilized than (**1t**, BF_4^-) and (**1t**, PF_6^-) by 20−25 kcal/mol in the gas phase and by ca. 15−17 kcal/mol in THF and acetone solution (see Table 2). These differences would anticipate K_{BPh_4} values significantly smaller than K_{BF_4} and K_{PF_6}, which is not in agreement with the values of the same order of magnitude derived from the kinetic data. A possible explanation for the additional stabilization of the BPh_4^- ion pairs in the experimental system is the possibility of stacking interactions with the phenyl groups in the dppe ligand not considered in the theoretical model. A second major conclusion of the calculations

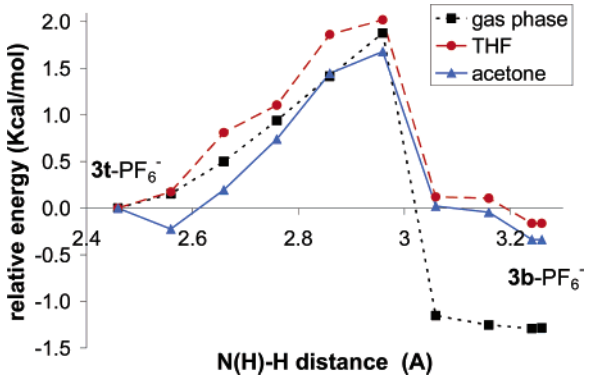

Figure 11. Potential energy curve for the **3t**-PF_6^- → **3b**-PF_6^- process taking the N···H—Fe distance as the reaction coordinate.

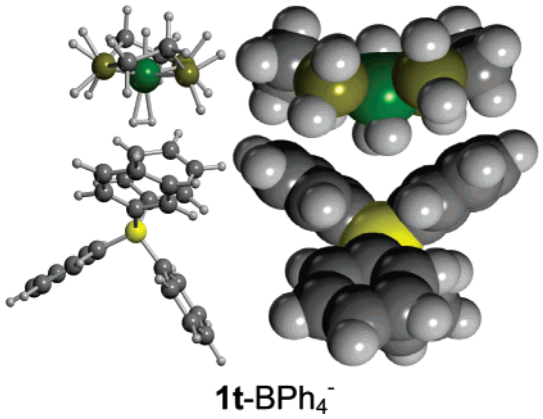

Figure 12. Structure of the ion pair (**1t**, BPh_4^-) in ball-and-stick and space-filling representations.

is the special geometry adopted by the (**1t**, BPh_4^-) ion pair (see Figure 12). Whereas the anions in (**1t**, BF_4^-) and (**1t**, PF_6^-) leave free space around the dihydrogen ligand and allow the subsequent attack by the base, the BPh_4^- in (**1t**, BPh_4^-) blocks the dihydrogen ligand and hinders deprotonation. Thus, in the presence of an excess of BPh_4^-, the complex will exist mainly in the form of BPh_4^- ion pairs, but deprotonation can only proceed through the small fraction of the metal complex existing either as a free complex or as an ion paired to the less abundant BF_4^- anion. As a consequence, the process is decelerated. Nevertheless, it must be also pointed out that BPh_4^- also stabilizes the final species in the reaction coordinate (**4t**, **5t**), so that its kinetic effect must be exclusively associated to the fact that the steric blockage of the H_2 ligand in the (**1t**, BPh_4^-) ion pairs avoids the existence of the key intermediates **2t** and **3t**.

Conclusion

Despite the fact that many reactions in inorganic and organometallic chemistry are carried out in solvents that favor the formation of ion pairs, their effect is not usually taken into account. The results in the present paper clearly illustrate the relevance of ion pair formation to the reactivity of the dihydrogen complex *trans*-[FeH(H_2)dppe$_2$]$^+$, which adds to other recent studies in which effects associated to the presence of anions in solution have been recognized for several systems.[5] The kinetic studies indicate that the rate of deprotonation of the dihydrogen complex with NEt_3 is largely affected by the presence of an excess of the BF_4^-, PF_6^-, and BPh_4^- anions. Although all three anions form ion pairs with a similar stability,

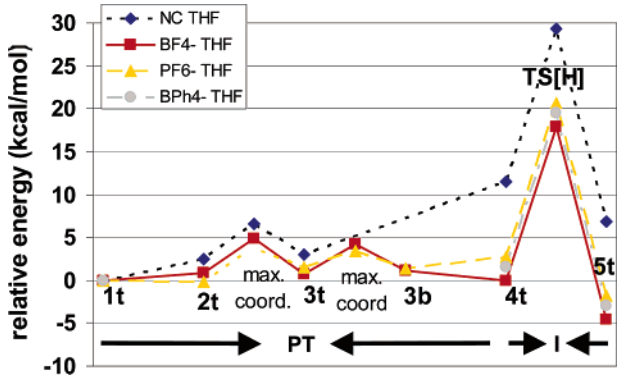

Figure 13. Energy profile in THF for the complete proton transfer (**PT**) + isomerization (**I**) process. The energy of complexes (**1t**, A^-) + NMe_3 has been taken as zero energy (A^- = NC, BF_4^-, PF_6^-, and BPh_4^- and NC = no counteranion).

the BF_4^- and PF_6^- ion pairs provide a more efficient reaction pathway for deprotonation than that going through the unpaired metal complex, whereas the BPh_4^- ion pairs are unproductive and represent a dead-end in the reaction mechanism. These observations are in agreement with the results of theoretical calculations, which provide additional information about the proton transfer and isomerization processes. With regards to the energetics of reaction of *trans*-[FeH(H_2)(dppe)$_2$]$^+$ with the base, Figure 13 summarizes the results obtained in THF. A very similar energy profile is obtained in acetone (see Supporting Information). As pointed out in previous sections, an important point for this reaction is the order of occurrence of the proton transfer and isomerization steps. In this sense, Figure 13 illustrates clearly that the activation barrier for the overall process through the pathways involving ion pairs is significantly smaller than the activation barrier found for the isomerization of the starting *trans*-hydride−dihydrogen complex (ca. 32 kcal mol^{-1}, see Table 1), thus confirming that proton transfer will preferentially occur first. On the other hand, it must be noted that, for the ineffective reaction pathway going through the unpaired metal complex, the energy barrier for the conversion of reactants to products includes significant contributions from both the proton transfer and the isomerization processes, so that the rate of reaction through this pathway must be expected to be too slow to make it competitive with the more efficient pathways going through ion pairs. In contrast, for reaction through the BF_4^- and PF_6^- ion pairs, there is an almost complete disappearance of the energy cost associated with the proton transfer step, so that this step can be considered to occur under conditions of reversible pre-equilibrium. In addition, Figure 13 indicates that the proton transfer step is less favored for the PF_6^- ion pairs than for the BF_4^- pathway, which is in agreement with the relative rates of reaction measured for both anions. As indicated in previous sections, the relative values in THF and acetone solutions of the rate constants for the pathways involving both anions can also be rationalized on the basis of the theoretical calculations.

For steric reasons, ion pairs with BPh_4^- are unable to evolve to the final reaction products, and so they are unable to provide a pathway equivalent to those provided by the other anions. It is also important to note that in addition to the kinetic effect, ion pairing also introduces an additional favorable thermodynamic contribution, mainly associated to the formation of ($HNEt_3^+$, X^-) ion pairs as reaction products. This contribution makes the overall process change from being disfavored for

the free metal complex to being favored for the ion pairs. As expected, it strongly depends on the nature of both the anion and the solvent, reaching a maximum for BF_4^- in THF where it represents a stabilization of 11.5 kcal/mol.

From a structural point of view, the reaction can be described as going through a series of dihydrogen bonded intermediates, which adds further support to the conclusions of previous works for related proton transfers,[8−11] mainly derived from studies of the reaction in the reverse sense (i.e., protonation of metal hydrides to form dihydrogen complexes). Nevertheless, an unprecedented intermediate structure that can be described as a complex containing an end-on coordinated dihydrogen has been located along the reaction coordinate. No significant structural differences exist for the intermediates formed in the reaction of the free metal complex with respect to those formed in the presence of BF_4^- or PF_6^-, the anion always following the metal complex and facilitating separation of the reaction products without any interference from the deprotonation process (i.e., ion pairing and dihydrogen bonding coexist and operate in a cooperative way for this system). This result contrasts with recent observations[18] showing that ion pairing with BF_4^- causes a deceleration of the proton transfer from HCl to the $[W_3S_4H_3(dmpe)_3]^+$ hydride complex. In that case, theoretical calculations indicate that BF_4^- can insert itself between the coordinated hydride and the acid, thus hindering formation of the dihydrogen bond required for the proton transfer. The observation of such a different behavior of the same anion in two related reactions indicates that more work must be made to achieve a precise understanding of the role of ion pairs in this kind of reaction.

Experimental Procedures

The complex *trans*-$[FeH(H_2)(dppe)_2](BF_4)$ was prepared following the literature procedure,[19] and its purity was confirmed by ^1H and $^{31}P\{^1H\}$ NMR. The formation of *cis*-$[FeH_2(dppe)_2]$ as the product of reaction with an excess of NEt_3 was also confirmed using NMR. All synthetic and kinetic work was carried out under an argon atmosphere using standard Schlenk procedures.

Kinetic experiments were made at 25.0 ± 0.1 °C using an Applied Photophysics SX18 stopped-flow instrument. The experiments were carried out by mixing a solution (THF or acetone) of *trans*-$[FeH(H_2)(dppe)_2](BF_4)$ (ca. 1.0×10^{-3} M) with another one containing a large excess of NEt_3 in the same solvent, so that pseudo-first-order conditions of base excess were always maintained. For kinetic measurements in the presence of added salts, the salts were added to the solution containing the base. The actual concentrations of base and salt are those shown in the Results and Discussion and in the tables in the Supporting Information. All solutions used in the kinetic work were prepared and transferred to the stopped-flow instrument under an argon atmosphere, and they were always used within the first 3−4 h from preparation. Preliminary experiments aimed at locating the wavelength showing the maximum absorbance changes were carried out with a PDA.1 diode array detector, which allowed determining that the reaction occurs in a single kinetic step. These experiments were also used to determine the first-order dependence of the observed rate constants with respect to the metal complex by checking that there were no changes of the rate constant with the complex concentration. As the preliminary experiments showed that the largest absorbance changes occurred at 380 nm, this wavelength was selected for monitoring the reaction kinetics under different experimental conditions. Kinetic data were analyzed using the SPECFIT/32 program[30] (diode array data) and the standard software of the stopped-flow instrument (single wavelength data). The values of the pseudo-first-order rate constants in both solvents using different concentrations of base and salt are given in the Supporting Information as the mean value of at least four separate measurements, the standard deviation always being significantly lower than 5%. The values of the second-order rate constants given in the text were derived from the fit of the corresponding pseudo-first-order constants, the reported standard deviation being in this case that corresponding to the fit.

Computational Details. Calculations were performed with the Gaussian 98 series of programs.[31] Density functional theory (DFT) was applied with the B3LYP functional.[31−34] Effective core potentials (ECPs) were used to represent the innermost electrons of the iron atom as well as the electron core of the phosphorus atoms.[35,36] The basis set for the Fe and P atoms was that associated with the pseudo-potential,[30,31] with a standard double-ξ LANL2DZ contraction, supplemented in the case of P with a set of d polarization functions.[37] A 6-31G(d,p) basis was used for hydrogen atoms directly bonded to the metal and the nitrogen and fluorine atoms, while a 6-31G basis set was used for the rest of atoms in the system.[38−40] The transition states for the isomerization processes were characterized by analytical frequency calculations.

The inclusion of solvent is mandatory to obtain realistic values of the ion pair energies. Solvent effects were taken into account by means of polarized continuum model (PCM) calculations[41,42] using standard options.[31] Free energies of solvation were calculated with THF ($\epsilon = 7.6$) and acetone ($\epsilon = 20.7$) as solvents, keeping the geometry optimized for the gas-phase species (single point calculations). The proton transfer and separation processes could be strongly affected by the solvent. Given the impossibility of locating the transition states in solution for technical reasons, our strategy has been to compute potential energy curves in the gas phase and then recalculating the complete curve with the solvent, instead of only performing single point calculations in solution for the gas-phase transition states. In this way, different positions of the transition state as a function of the nature of the solvent can be taken into account. The curves presented in Figures 5, 6, 8, 9, and 11 have been obtained with this approach.

Acknowledgment. Financial support from the Spanish MEC trough Projects BQU2003-04737 and CTQ2005-09000-C02-01, from the Generalitat de Catalunya through Grant 2005SGR00896, and from Junta de Andalucia with Ayuda a Grupos FQM-137 is gratefully acknowledged. A.L. thanks the Generalitat de Catalunya for a "Distinció per a la Promoció de la Recerca Universitària". The use of the computational facilities at the Centre de Supercomputació de Catalunya (CESCA) is appreciated as well.

Supporting Information Available: Tables including the values of rate constants; energy profile summarizing the results obtained in acetone solvent; complete ref 31; and Cartesian coordinates and absolute energies for all computed minima and transition states. This material is available free of charge via the Internet at http://pubs.acs.org.

JA070939L

(30) Binstead, R. A.; Jung, B.; Zuberbühler, A. D. *SPECFIT*/32; Spectrum Software Associates: Chapel Hill, NC, 2000.

(31) Frisch, M. et al. *Gaussian 98*; Gaussian Inc.: Pittsburgh, PA, 1998.
(32) Lee, C. T.; Yang, W. T.; Parr, R. G. *Phys. Rev. B* **1988**, *37*, 785−789.
(33) Becke, A. D. *J. Chem. Phys.* **1993**, *98*, 5648−5652.
(34) Stephens, P. J.; Devlin, F. J.; Chabalowski, C. F.; Frisch, M. J. *J. Phys. Chem.* **1994**, *98*, 11623−11627.
(35) Hay, P. J.; Wadt, W. R. *J. Chem. Phys.* **1985**, *82*, 299−310.
(36) Wadt, W. R.; Hay, P. J. *J. Chem. Phys.* **1985**, *82*, 284−298.
(37) Hollwarth, A.; Bohme, M.; Dapprich, S.; Ehlers, A. W.; Gobbi, A.; Jonas, V.; Kohler, K. F.; Stegmann, R.; Veldkamp, A.; Frenking, G. *Chem. Phys. Lett.* **1993**, *208*, 237−240.
(38) Hehre, W. J.; Ditchfie, R.; Pople, J. A. *J. Chem. Phys.* **1972**, *56*, 2257−2261.
(39) Hariharan, P. C.; Pople, J. A. *Theor. Chim. Acta* **1973**, *28*, 213−222.
(40) Francl, M. M.; Pietro, W. J.; Hehre, W. J.; Binkley, J. S.; Gordon, M. S.; Defrees, D. J.; Pople, J. A. *J. Chem. Phys.* **1982**, *77*, 3654−3665.
(41) Amovilli, C.; Barone, V.; Cammi, R.; Cances, E.; Cossi, M.; Mennucci, B.; Pomelli, C.; Tomasi, J. In *Advances in Quantum Chemistry, Vol. 32*; Wilson, S., Marvani, J., Grout, P. J., McWeeny, R., Smeyers, Y. G., Eds.; Academic Press: San Diego, CA, 1999.
(42) Tomasi, J.; Persico, M. *Chem. Rev.* **1994**, *94*, 2027−2094.